Asian Journal of Chemistry; Vol. 25, No. 10 (2013), 5805-5810

ASIAN JOURNAL OF CHEMISTRY

http://dx.doi.org/10.14233/ajchem.2013.OH97

Performance of C,N-Impregnated Photocatalyst Coupled with Continuous-Flow Reactor for Removal of Gaseous Aromatic Pollutants†

WAN-KUEN JO* and HYUN-JUNG KANG

Department of Environmental Engineering, Kyungpook National University, 80 University Road, Bukgu, Daegu 702-701, Republic of Korea

*Corresponding author: Fax: +82 53 9506579; Tel: +82 53 9506584; E-mail: wkjo@knu.ac.kr

AJC-13340

Previous activity tests of carbon and nitrogen co-impregnated photocatalysts (C and N-impregnated-TiO_2) for environmental pollution controls were primarily performed in the aqueous phase to investigate the decomposition of water pollutants. This study examined the photocatalytic activities of C,N-TiO_2 photocatalysts for the purification of indoor-level gaseous organic compounds under different experimental conditions. The as-prepared C,N-TiO_2 and unmodified TiO_2 powders were characterized using XRD, SEM, diffuse reflectance UV-VIS-NIR spectra and Fourier transform infrared spectra. The C,N-TiO_2 powders exhibited a shift in the absorbance spectrum towards the visible light region when compared to TiO_2 powders, indicating that the as-prepared C,N-TiO_2 photocatalyst could be effectively activated by visible-light irradiation. The surface characteristics of the two types of photocatalysts differed. Additionally, the average photocatalytic degradation efficiencies for benzene, toluene, ethyl benzene and xylene (BTEX) obtained from the C,N-TiO_2 system were 27, 81, 95 and 99 %, respectively, whereas those of the TiO_2 powders were close to zero, 19, 47 and 56 %, respectively. Under the experimental conditions used in this study, the photocatalytic degradation efficiencies for BTEX were higher for the photocatalytic system with the fluorescent lamp than for that with light-emitting diodes.

Key Words: Degradation efficiency, Operational condition, Aromatic pollutant, Light-emitting diode.

INTRODUCTION

Nonmetallic nitrogen (N)- or carbon (C)-impregnated TiO_2 nanophotocatalysts have been found to have superior photocatalytic activity under visible-light irradiation due to effective narrowing of the energy band gap of TiO_2[1,2]. The shift in the absorption band toward the visible-light region for N-impregnated TiO_2 can be attributed to the N-induced mid-gap energy (N 2p) state, which was formed slightly above the top of the valence band (O 2p)[3] or narrowing of the band gap by mixing the N 2p and O 2p states in the valence band[4]. The carbon dopant has been described as a substitutional anion associated with the -4 oxidation state in the Ti-C bond in carbide, or as an interstitial cation associated with the +4 oxidation state in the C-O bond in carbonates[5]. These oxidation states are attributed to the band gap narrowing of TiO_2 or the formation of a localized mod-gap state, thereby extending the absorbance of C-TiO_2 into visible light[6]. C-TiO_2 also reduces the electron-hole recombination which in practice reduces the effectiveness of TiO_2 as a photocatalyst[7].

More recently, co-impregnation of TiO_2 with carbon and nitrogen (C,N-TiO_2) has been suggested as an alternative technique to effectively extend the absorbance into visible light with a higher photocatalytic activity over single element doping into TiO_2[8,9]. This was ascribed to a synergistic effect of co-impregnation with the two elements in which the impregnated C atoms would increase adsorption of chemicals and the impregnated N atoms would enhance the visible-light absorption. A number of researchers have synthesized C,N-TiO_2 photocatalysts using various routes such as solvothermal[10], mechanochemical[11], hydrolysis-polymerization-calcination[12], hydrothermal[9] and sol-gel processes[13] and found that as-prepared C,N-TiO_2 photocatalysts exhibited high photocatalytic activities under visible-light irradiation. For these studies, the photocatalytic activity tests were carried out in the aqueous phase to examine the decomposition of water pollutants, such as phenol and methylene blue, or inorganic gas (nitrogen monoxide). However, it is worth noting that both photon absorbance kinetics and reaction kinetics of environmental pollutants differ at the liquid-solid and gas-solid interfaces[14]. This difference prompts assessment of the photocatalytic activities of as-prepared C,N-TiO_2 photocatalysts for the removal of gas-phase pollutants.

This study investigated the photocatalytic activities of C,N-TiO_2 photocatalysts for the purification of indoor-level

†Presented to the 6th China-Korea International Conference on Multi-functional Materials and Application, 22-24 November 2012, Daejeon, Korea

gaseous organic compounds under different experimental conditions. The photocatalysts were prepared using a versatile solvothermal synthetic method. In addition, the photocatalytic activities of commercially-available Degussa P-25 TiO_2 powders were compared with those determined for the as-prepared C,N-TiO_2 powders. The target compounds included benzene, toluene, ethyl benzene and xylene (BTEX), which are commonly detected at high concentrations in indoor and outdoor environments[15]. Moreover, these compounds are toxic or potentially toxic to humans[16].

EXPERIMENTAL

Synthesis and characterization of C,N-TiO_2 photocatalysts: The C,N-TiO_2 photocatalysts were prepared using a solvothermal method. For this method, titanium isopropoxide (TTIP, 4.8 mL) was added to 68 mL of isopropanol. This solution was mixed with 4 mL of HNO_3 (0.5 M) and 0.78 g of hexamethylenetetramine (HMT) and then stirred for 1 h at room temperature to obtain a gel-type photocatalyst. Subsequently, the gel-type photocatalyst was transferred into a 100 mL Teflon-lined stainless steel autoclave and then heated at 120 ºC for 4 h. After thermal treatment was completed the autoclave was cooled and then kept at room temperature for 20 h. The resulting C,N-TiO_2 photocatalysts were dried at 90 ºC for 24 h and then calcined at 300 ºC for 4 h.

The as-prepared C,N-TiO_2 and un-impregnated TiO_2 powders were characterized using X-ray diffraction, scanning emission microscope, diffuse reflectance UV-VIS-NIR analysis and Fourier transform infrared (FTIR) analysis. XRD patterns were determined on a Rigaku D/max-2500 diffractometer with CuK_α radiation operated at 40 kV and 100 mA in the range of 20-80o (2θ) at a scanning rate of 10º min^{-1}. The particle morphology was observed using a Hitachi S-4300 and EDX-350 FE-SEM at an acceleration voltage of 15 kV. Visible absorption spectra were obtained for the dry pressed disk samples using a Varian CARY 5G spectrophotometer equipped with an integrating sphere. Polytetrafluoroethylene was used as a reference. FTIR analysis was performed on a PerkinElmer Spectrum GX spectrophotometer at a resolution of 4 cm^{-1} in the spectral range of 4000-400 cm^{-1}, using a KBr pellet for sample preparation.

Photocatalytic activity test: The photocatalytic activity of the prepared C,N-TiO_2 and unmodified TiO_2 photocatalysts was examined using an annular-type Pyrex reactor with a dimension of 5.2 cm inside diameter and 26 cm length. The as-prepared C,N-TiO_2 or unmodified TiO_2 powders were coated onto the inner surface of the Pyrex reactor. Air leakage from the reactor was determined by measuring the flow rate at the reactor outlet and comparing this with the supply airflow rate. Visible radiation was supplied using a conventional visible-light lamp or visible light-emitting diodes and its intensity was measured using a digital Lux Meter (INS Model DX-100). The reactor outside was wrapped with aluminum foil to minimize the transmission loss of light from the reactor lamp through the Pyrex tube, as well as for the transmission gain of light from laboratory fluorescent lamps. This reactor allows for a uniform light distribution onto the surfaces of the photocatalysts. In addition, the reactor was designed to direct the flow of incoming air toward the UV light to increase air turbulence inside the reactor, thereby enhancing distribution of the target compounds onto the photocatalyst surface. The standard gas, which was prepared by injecting standard gases into a mixing chamber via a syringe pump (model 210, KdScientific Inc.), flowed above the C,N-TiO_2-coated Pyrex. The humidity was adjusted by passing zero-grade air through a charcoal filter, followed by a humidifying device in a water bath. SFR was controlled using rotameters calibrated against a dry test meter. The RH values were measured immediately adjacent to the photocatalytic reactor inlet using a humidity meter (Thermo Recorder TR-72S, T & D Co.)

This study investigated the effect of light sources on the destruction efficiency of BTEX. Visible radiation was supplied by an 8-W fluorescent daylight lamp (F8T5DL, Youngwha Lamp Co.) or blue light-emitting diodes with a peak light intensity at 470 nm. Other parameters were fixed to their representative values, which were as follows: lamp, 8-W fluorescent daylight lamp; RH, 45 %; IC, 0.1 ppm; SFR, 0.5 L min^{-1}. The representative hydraulic diameter (HD is defined as the inside diameter of the annular reactor tube minus the outside diameter of the lamp) of the photocatalytic reactor was 35 mm. The visible radiation intensity was measured as 2.1 mW cm^{-2} at a distance from the visible-light lamp equal to half the HD of the reactor. The weight of the C,N-impregnated TiO_2 and un-impregnated TiO_2 film coated inside the reactor were 3.4 and 3.5 mg cm^{-2}, respectively.

Sampling and analysis: Gas samples were collected at both the inlet and outlet using an empty Tedlar bag at a constant flow rate for 10 min every hour. Gas from the sampling bag was then drawn through a adsorbent trap containing 0.2 g of Tenax TA using a constant flow-sampling pump (Aircheck Sampler Model 224-PCXR8, SKC). All sampling was conducted at ambient temperature. The target species collected on the adsorbent trap were analyzed by coupling a thermal desorption system (SPIS TD, Donam Inc.) to a gas chromatograph (Agilent 7890A) equipped with a flame ionization detector. The peak areas with respect to other compounds on the GC chromatogram were not significantly high and the could not be easily assigned to theoretically expected intermediates; thus, they were not quantified.

The quality assurance and quality control program for measurements of gaseous target compounds included laboratory blank traps and spiked samples. At the beginning of the day, a laboratory blank trap was analyzed to check for any trap contamination. However, none was observed. An external standard was also analyzed daily to check the quantitative response. When the quantitative response differed by more than 10 % from that predicted by the specified calibration equation, a new calibration equation was determined. The method detection limits ranged from 1.5 to 5.2 μg m^{-3}, depending on the target volatile organic compounds.

RESULTS AND DISCUSSION

Characteristics of C,N-TiO_2 and un-impregnated TiO_2 photocatalysts: The prepared C,N-TiO_2 powders and the TiO_2 Degussa P25 powders were characterized by XRD, SEM, UV-visible spectroscopy and FTIR analysis. Fig. 1 exhibits the

XRD patterns of C,N-TiO_2 and unmodified TiO_2 Degussa P25. The XRD results of unmodified titania exhibited an anatase phase of TiO_2 with a major peak at 25.2º 2θ and a rutile phase with a distinct peak at 27.4º 2θ. These findings are similar to those of previous studies[17,18]. However, C,N-TiO_2 did not reveal any distinct rutile crystal phase peak at 27.4 2θ, although it still showed a distinct anatase crystal phase peak at 25.2º 2θ. Moreover, unlike the unmodified TiO_2 no distinct anatase peaks were observed for the C,N-TiO_2. These findings are consistent with those of previous studies[9,10,12,13]. The differences in XRD patterns between unmodified TiO_2 and C,N-TiO_2 were ascribed to the calcination temperature of C,N-TiO_2 and the role of C and N elements for C,N-TiO_2. Previous studies[10,12,13] showed that crystallinity transformations from rutile TiO_2 to anatase TiO_2 occur during calcination processes and that these transformations increase as calcination temperature increases. The presence of C and N elements for C,N-TiO_2 could also influence the phase transformation[12].

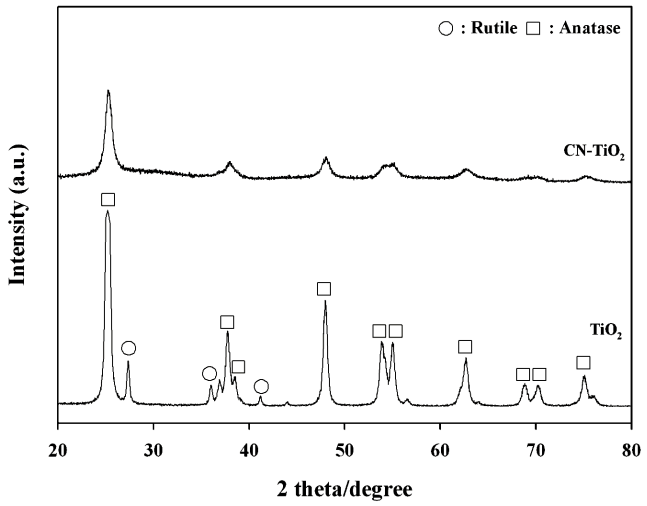

Fig. 1. X-ray diffraction spectra of C,N-TiO_2 and TiO_2 powders

The SEM images of both C,N-TiO_2 and unmodified TiO_2 Degussa P25 are presented in Fig. 2. Lower agglomeration was observed for the C,N-TiO_2 than for the unmodified sample. The average sizes of the agglomerate for C,N-TiO_2 and unmodified TiO_2 were *ca*. 10 and 20 nm, respectively, which are consistent with the results reported by Wang and Lim[10]. The larger size of C,N-TiO_2 when compared to the unmodified TiO_2, is supported by Wang and Lim[10], who reported that the crystallite size increased as the crystallinity transformation from rutile TiO_2 to anatase TiO_2 occurred. Additionally, the C,N-TiO_2 showed more aggregation of particles when compared to unmodified TiO_2. These findings are attributed to the sintering reaction among small particles for the C,N-TiO_2[19]. However, it should be noted that the particle size of C,N-TiO_2 photocatalysts can vary with calcination temperature[12,13].

The UV-visible absorbance spectra of the two photocatalysts are presented in Fig. 3. The P25 TiO_2 revealed an absorption edge at $\lambda \approx$ 410 nm, which was consistent with that reported by other researchers[17,20,21]. The light absorbance intensity in the UV region (< 400 nm) was higher for unmodified TiO_2 than for C,N-TiO_2. However, unlike the unmodified TiO_2, the C,N-TiO_2 powders showed a shift of the absorbance spectrum towards the visible light region (400-800 nm). Similarly, previous studies[9,13,22] reported that the C,N-TiO_2 prepared using other synthetic routes (sol-gel, magnetron sputtering and hydrothermal methods) showed a light absorbance shift to the visible light region, although their absorbance intensities differed. Taken together, these findings indicate that the C,N-TiO_2 powders prepared in this study could be effectively activated by visible-light irradiation.

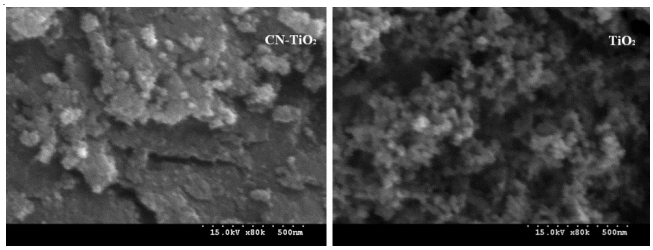

Fig. 2. Scanning electron microscope pattern of C,N-TiO_2 and TiO_2 powders

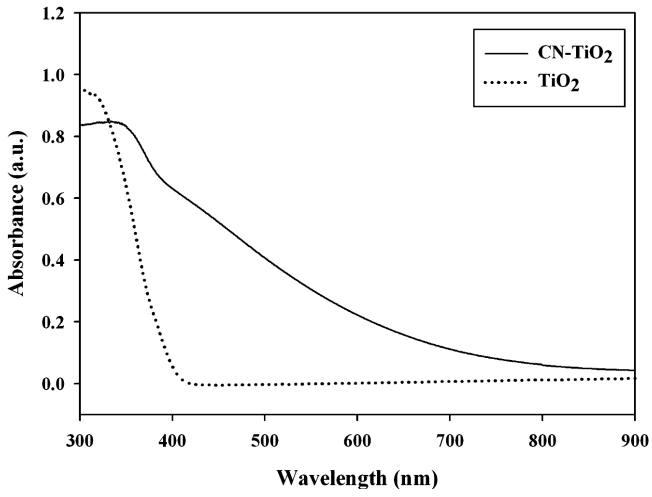

Fig. 3. UV-visible absorption spectra of C,N-TiO_2 and TiO_2 powders

Fig. 4 shows the FTIR spectra of the prepared C,N-TiO_2 and unmodified TiO_2 Degussa P25 powders. Major peaks were observed at 3411, 1630 and < 1000 cm^{-1} (Fig. 3), which is similar to the results reported by Dolat *et al.*[9]. The band at 3411 cm^{-1} was attributed to O-H stretching vibration, while the band at 1630 cm^{-1} area was ascribed to O-H bending of water molecules absorbed onto the catalyst surface[9,18]. The bands at 460 and 694 nm were assigned to the stretching vibration of Ti-O[18]. The spectra of C,N-TiO_2 did not show additional peaks when compared to the spectra of unmodified TiO_2. However, for the peak at < 1000 cm^{-1} the frequency was shifted from 694 nm for TiO_2 to 460 nm for C,N-TiO_2. This frequency movement to a lower wavelength for C,N-TiO_2 was attributable to the interaction between the impregnated C and N[9].

Comparison of photocatalytic activities between C,N-TiO_2 and unmodified TiO_2 systems: The photocatalytic activities of a C,N-TiO_2 composite for cleaning of gaseous aromatic compounds (BTEX) were examined under a variety of operational conditions. Furthermore, the photocatalytic activities of commercial titania (Degussa P25 TiO_2) were compared to those of the C,N-TiO_2. Fig. 5 shows the average degradation efficiencies for all compounds determined using

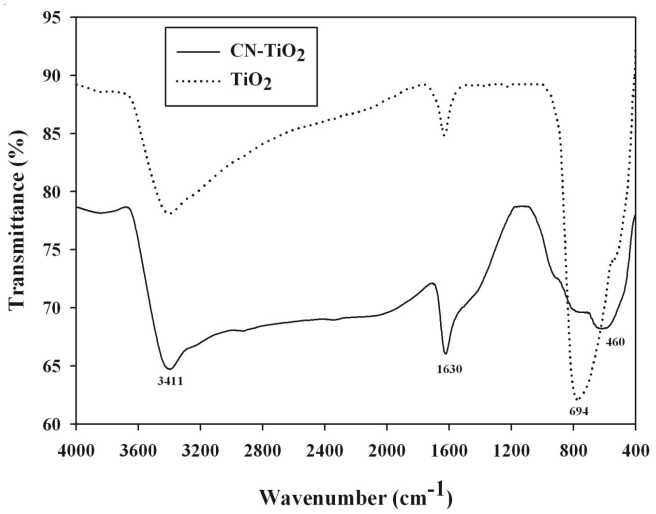

Fig. 4. Fourier transform infrared spectra of C,N-TiO_2 and TiO_2 powders

the C,N-TiO_2 and commercial TiO_2 under visible-light irradiation. The decomposition efficiencies obtained from the C,N-TiO_2 photocatalytic system were higher than those of the TiO_2 system. The average photocatalytic degradation efficiencies for BTEX obtained from the C,N-TiO_2 system were 27, 81, 95 and 99 %, respectively, whereas those of the TiO_2 powders were close to zero, 19, 47 and 56 %, respectively. These findings indicate that the C,N-TiO_2 photocatalyst was superior for photocatalytic decomposition of toxic gas-phase aromatic pollutants to the reference Degussa P25 TiO_2 photocatalyst under visible-light irradiation. In turn, this identification supports the assertion that C and N elements embedded into TiO_2 networks could enhance the visible-light absorbance of TiO_2 and therefore its photocatalytic activities. These findings are similar to those of other studies[11,19,23], in which C,N-TiO_2 exhibited enhanced photocatalytic activities for the degradation of water-based or inorganic gas pollutants. This enhanced photocatalytic activity of the C,N-TiO_2 photocatalyst was ascribed to the combined effect of C and N atoms in the TiO_2 networks. Previous studies[11,19,23] suggested that C atoms could act as a photosensitizer, which transfers excited electron to surface-adsorbed oxygen molecules to form reactive O_2^-, thereby initiating the degradation of chemicals. Moreover, N atoms might produce low energy levels of N 2p and O 2p states or introduce a mid-gap (N 2p) energy level.

Photocatalytic decomposition efficiencies according to lamp type: The photocatalytic activities of a C,N-TiO_2 photocatalyst were evaluated for degradation of BTEX using two different light sources (8-W fluorescent daylight lamp and violet visible light-emitting diodes). As shown in Fig. 6, the photocatalytic degradation efficiencies for BTEX were higher for the photocatalytic system with the fluorescent lamp than

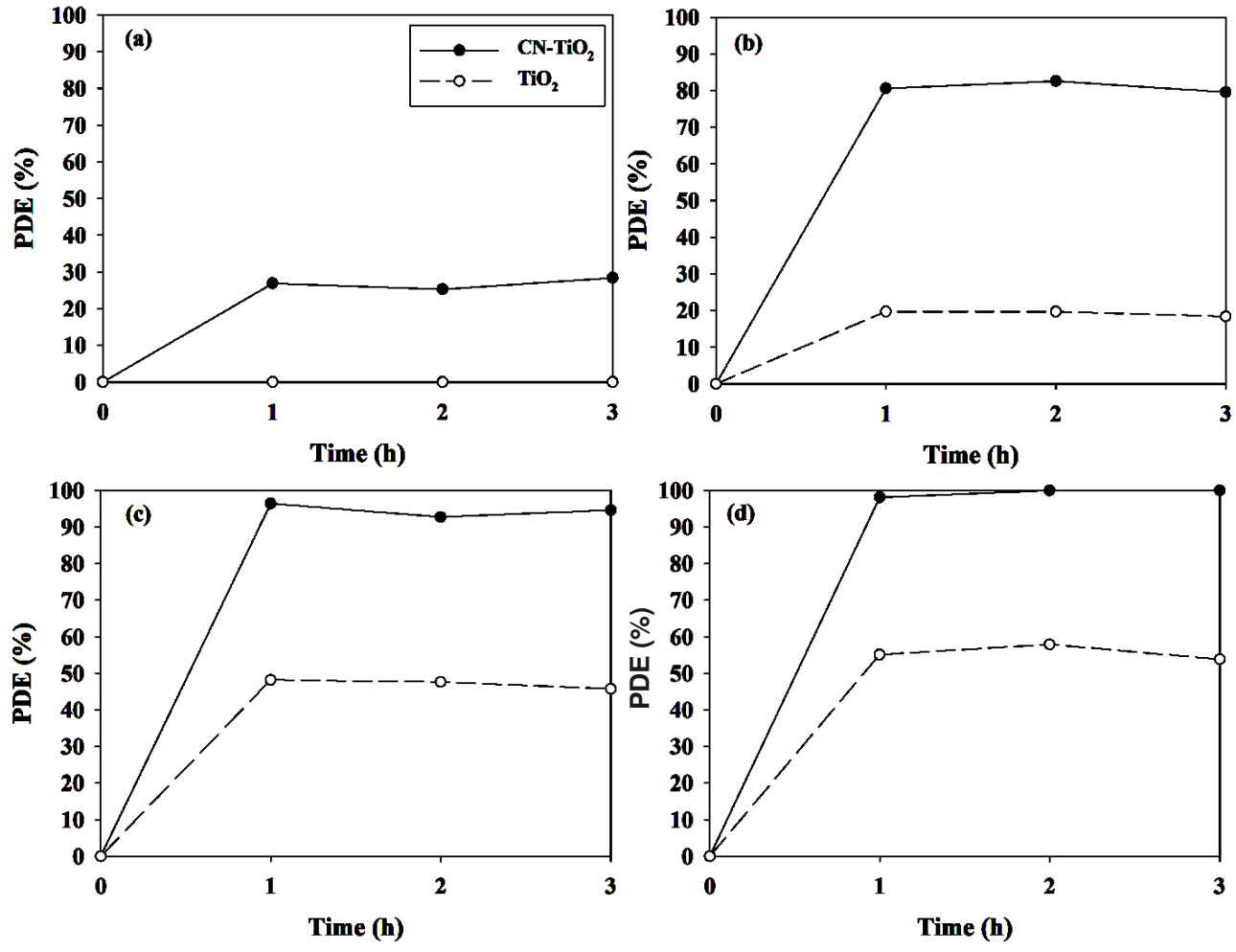

Fig. 5. Comparison of photocatalytic decomposition efficiencies (PDEs) of (a) benzene, (b) toluene, (c) ethyl benzene, and (d) *o*-xylene between C,N-TiO_2 and unmodified TiO_2 photocatalytic systems

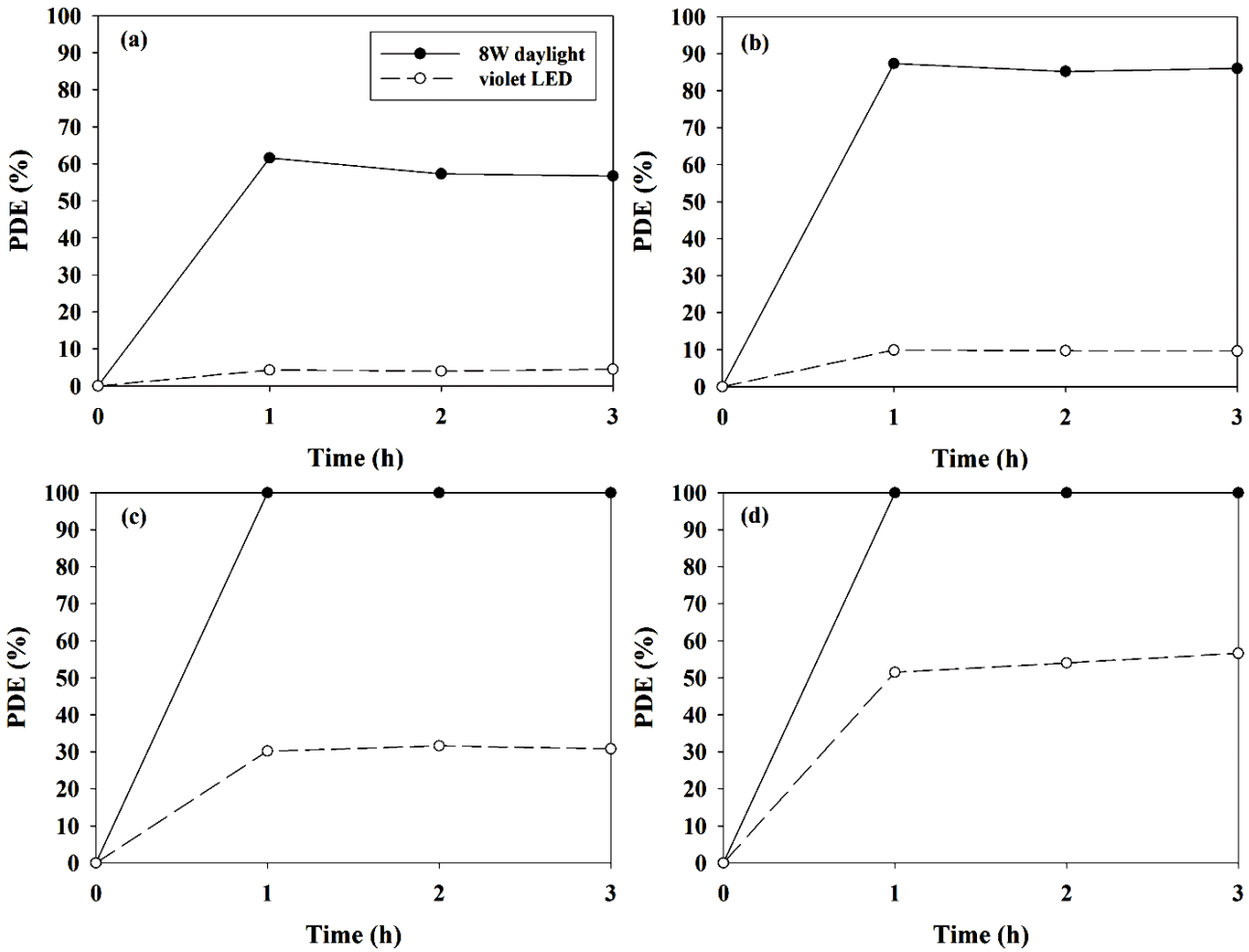

Fig. 6. Photocatalytic decomposition efficiencies (PDEs) of (a) benzene, (b) toluene, (c) ethyl benzene, and (d) *o*-xylene determined *via* a photocatalytic system with C,N-TiO_2 and TiO_2, according to lamp type

for that with light-emitting diodes. The average degradation efficiencies for BTEX obtained from the former system were 59 and 86 %, close to zero and close to zero, respectively, whereas those of the latter system were 4, 10, 31 and 54 %, respectively. Photocatalytic degradation efficiency is proportional to light intensity[24]. The fluorescent lamp exhibited lower light intensity (1.6 mW cm^{-2}) than that of the light-emitting diodes (0.2 mW cm^{-2}), indicating that light intensity was an important factor for the difference in degradation efficiencies between the fluorescent lamp and light-emitting diodes under the experimental conditions used in the present study. Moreover, the light wavelength of fluorescent lamp was distributed at a wide range of 400-720 nm, which comprised lower wavelengths than that of the light-emitting diodes. Thus, the elevated degradation efficiency for the fluorescent lamp/C,N-TiO_2 system was attributed to higher light absorbance by C,N-TiO_2 powders at a low wavelength, as shown previously in the UV-visible spectra (Fig. 3). In addition, the power supplied by the fluorescent lamp was 8 W, whereas it was 1.9 W for the light-emitting diodes, suggesting that a higher power supplied by the fluorescent lamp would also result in elevated removal efficiencies for BTEX. Other studies[25,26] have also reported that a conventional 8-W fluorescent lamp exhibited higher photocatalytic activities for degradation of gaseous dimethyl sulfide or formaldehyde, but that light-emitting diodes could still be utilized as energy-efficient alternative light sources for the photocatalytic systems.

Conclusion

This work explored the photocatalytic activities of C,N-TiO_2 photocatalysts for the purification of indoor-level gaseous BTEX under different conditions. The surface characteristics of the as-prepared C,N-TiO_2 photocatalysts differed from those of the Degussa P25 TiO_2 photocatalyst. In particular, the C,N-TiO_2 powders exhibited a shift in the absorbance spectrum towards the visible light region when compared to TiO_2 powders, indicating that the as-prepared C,N-TiO_2 photocatalyst could be effectively activated by visible-light irradiation. Another major finding was that the C,N-TiO_2 photocatalytic system showed superior BTEX decomposition efficiencies to unmodified TiO_2 under visible-light irradiations. Moreover, the effects of the photocatalytic activity of C,N-TiO_2 on the type of light sources were quantified.

ACKNOWLEDGEMENTS

This work was supported by the National Research Foundation of Korea (NRF) grant funded by the Korean Government (MEST) (No. 2011-0027916).

REFERENCES

1. S. Yin, Y. Aita, M. Komatsu, J. Wang, Q. Tang and T. Sato, *J. Mater. Chem.*, **15**, 674 (2005).
2. H. Li, D. Wang, H. Fan, P. Wang, T. Jiang and T. Xie, *J. Colloid Interf. Sci.*, **354**, 175 (2011).
3. T. Lindgren, J.M. Mwabora, E. Avendaño, J. Jonsson, A. Hoel, C.-G. Granqvist and S.-E. Lindquist, *J. Phys. Chem. B*, **107**, 5709 (2003).
4. R. Asahi, T. Morikawa, T. Ohwaki, K. Aoki and Y. Taga, *Science*, **293**, 269 (2001).
5. D. Valentin, C. Pacchioni and A. Selloni, *Chem. Matter.*, **17**, 6656 (2005).
6. X. Chen and C. Burda, *J. Am. Chem. Soc.*, **130**, 5018 (2008).
7. R. Leary and A. Westwood, *Carbon*, **49**, 741 (2011).
8. Y. Xie, Y. Li and X. Zhao, *J. Mol. Catal. A*, **277**, 119 (2007).
9. D. Dolat, N. Quici, E. Kusiak-Nejman, A.W. Morawski and G. Li Puma, *Appl. Catal. B*, **115-116**, 81 (2012).
10. X. Wang and T.-T. Lim, *Appl. Catal. B*, **100**, 355 (2010).
11. S. Yin, M. Komatsu, Q. Zhang, F. Saito and T. Sato, *J. Mater. Sci.*, **42**, 2399 (2007).
12. S. Zhang and L. Song, *Catal. Comm.*, **10**, 1725 (2009).
13. D. Chen, Z. Jiang, J. Geng, Q. Wang and D. Yang, *Ind. Eng. Chem. Res.*, **46**, 2741 (2007).
14. A. Fujishima, X. Zhang and D.A. Tryk, *Surf. Sci. Rep.*, **63**, 515 (2008).
15. T. Ohura, T. Amagai, X. Shen, S. Li, P. Zhang and L. Zhu, *Atmos. Environ.*, **43**, 6352 (2009).
16. C.S. Chen, Y.C. Hseu, S.H. Liang, J.-Y. Kuo and S.C. Chen, *J. Hazard. Mater.*, **153**, 351 (2008).
17. W.K. Jo and J.T. Kim, *J. Hazard. Mater.*, **164**, 360 (2009).
18. S.H. Nam, T.K. Kim and J.H. Boo, *Catal. Today*, **185**, 259 (2012).
19. C. Yu and J. Yu, *Catal. Lett.*, **129**, 462 (2009).
20. T. Horikawa, M. Katoh and T. Tomida, *Micropor. Mesopor. Mater.*, **110**, 397 (2008).
21. H. Znad and Y. Kawase, *J. Mol. Catal. A*, **314**, 55 (2009).
22. K.R. Wu and C.H. Hung, *Appl. Surf. Sci.*, **256**, 1595 (2009).
23. X. Yang, C. Cao, L. Erickson, K. Hohn, R. Maghirang and K. Klabunde, *J. Catal.*, **260**, 128 (2008).
24. T.H. Lim and S.D. Kim, *Chemosphere*, **54**, 305 (2004).
25. J.L. Shie, C.H. Lee, C.S. Chiou, C.T. Chang, C.C. Chang and C.Y. Chang, *J. Hazard. Mater.*, **155**, 164 (2008).
26. W.K. Jo, S.S. Eun and S.H. Shin, *Photochem. Photobiol.*, **87**, 1016 (2011).